



**ISLAMIC UNIVERSITY OF TECHNOLOGY
ORGANISATION OF ISLAMIC COOPERATION**



**STUDYING THE EFFECT OF VARIOUS CONTACT
MATERIALS IN PEROVSKITE/SILICON TANDEM SOLAR
CELL**

B.Sc. Engineering (Mechanical) Thesis

Authored by

SHAMAITA SHABNAM

Student ID: 160011061

SUPERVISED BY

PROF. DR. MD. HAMIDUR RAHMAN

Department of Mechanical and Production Engineering (MPE)

Islamic University of Technology (IUT)

**DEPARTMENT OF MECHANICAL AND PRODUCTION ENGINEERING
(MPE)**

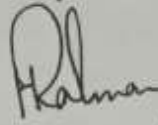
Islamic University of Technology (IUT)

MARCH, 2021

CERTIFICATE OF RESEARCH

This thesis titled "STUDYING THE EFFECT OF VARIOUS CONTACT MATERIALS IN PEROVSKITE/SILICON TANDEM SOLAR CELL" submitted by SHAMAITA SHABNAM (160011061), has been accepted as satisfactory in partial fulfillment of the requirement for the Degree of Bachelor of Science in Mechanical Engineering on March, 2021.

Supervisor

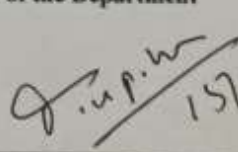


15/03/21

PROF. DR. MD. HAMIDUR RAHMAN

Department of Mechanical and Production Engineering (MPE)
Islamic University of Technology (IUT)

Head of the Department



15/03/2021

PROF. DR. MD. ANAYET ULLAH PATWARI

Department of Mechanical and Production Engineering (MPE)
Islamic University of Technology (IUT)

Candidate's Declaration

It is hereby declared that, their thesis or any part of it has not been submitted elsewhere for the award of any degree or diploma.

Signature of the Candidate's

Shamaita Shabnam

SHAMAITA SHABNAM

Student ID: 160011061

Department of Mechanical and Production Engineering (MPE)

Islamic University of Technology (IUT)

Board Bazar, Gazipur-1704

Dhaka, Bangladesh

Signature of the Supervisor

Rahman 16/03/21

PROF. DR. MD. HAMIDUR RAHMAN

Department of Mechanical and Production Engineering(MPE)

Islamic University of Technology(IUT)

Acknowledgments

I would like to express my sincere thanks to my respected supervisor Dr. Md. Hamidur Rahman sir, for his continuous support and guidance throughout this research period and my undergraduate study. His motivation and faith in me helped me in every step of my journey and in the completion of this thesis.

I am grateful to my parents for their encouragement and support at all times. Without their guidance my work would not have been possible. To my mother, I thank her for being there for me at all times. To my father, I am most grateful for lending me his own thesis book and encouraging me to improve on my work. Indeed they are a blessing to me.

I am most indebted to my fellow peers and friends who have been a constant support in all my efforts. I thank them for all the encouragement, for cheering me on, and for lending me a hand and an ear whenever I faced hurdles in the completion of my thesis, having no teammates to lean on. Especially to my roommate Hakim Dina Anjum, my constant go-to person, the girls of MCE'16, and to Md. Tanbir Sarowar, for his words of consolation, I express my deepest gratitude.

To Minhazul Alam Prottoy, my junior in the department of Mechanical and Production Engineering, I would like to acknowledge his enthusiasm in my work and thank him for suggesting this field of research to me. I pray for his success in his future endeavours.

Abstract

In the last decade, Perovskite based solar cells have seen massive enhancement, as opposed to conventional silicon (Si) based solar cells. As a result, its research has attracted a lot of attention in recent times. The material, still being under extensive research, has shown much changes in power conversion efficiency due to factors such as thickness, irradiance, temperature, and etcetera.

This thesis looks into the effect of different types of optical materials if used as contact materials on the open-circuit voltage, short-circuit current and power conversion efficiency, in the case of a perovskite/Si tandem solar cell. The software used for this study is GPVDM software. Built-in electrical parameters have been used in the simulation procedure and the materials changed within the layers to see the effect. The simulations utilised Maxwell-Boltzmann analysis to perform the task. The results show that the type of contact material affects the efficiency, and that different oxides give varying efficiencies. Metal contacts showed better performance when used as back contact, while oxides were more efficient on the front. The work also compares the performance of a tandem cell to the performance of a simple silicon base solar cell, where the results indicate improved performance for the tandem cells. This study will aid in understanding how perovskite/Si tandem cells behave in terms of its contact materials, so that more enhancement can be achieved and improved upon in further studies.

Keywords: *Perovskite, power conversion efficiency, contact materials, tandem solar cell, GPVDM*

Table of Contents

Abstract.....	v
List of Figures.....	vii
List of Tables.....	ix
Nomenclature and Abbreviations	x
Chapter 1 Introduction.....	1
1.1 Solar Cells.....	3
1.2 Solar Cell Structure and Operation.....	5
1.3 Tandem Solar Cells.....	9
Chapter 2 Literature Review	10
Chapter 3 Methodology.....	13
3.1 GPVDM.....	13
3.2 Validation.....	14
3.3 Modelling.....	20
Chapter 4 Result Analysis	26
Chapter 5 Summary and Conclusions	33
Chapter 6 Future Directions and Recommendations.....	34
References	35

List of Figures

Figure 1: A generic perovskite crystal structure of the form ABX_3	1
Figure 2: Power Conversion Efficiency by Year for various cell materials	2
Figure 3: Open-circuit Voltage for cell materials	3
Figure 4: Diagram of a solar cell structure	4
Figure 5: Solar panels installed on Satellite (Photo: NASA)	5
Figure 6: Rooftop solar panel in Bangladesh (Photo: Zahiduddin Saimon, Bangladeshpost.net).....	5
Figure 7: V_{oc} , J_{sc} , P_{max} on jv curve.....	6
Figure 8: Charge carriers under the influence of μ and τ	8
Figure 9: Parasitic components of a solar cell	8
Figure 10: Series connected tandem solar cell	9
Figure 11: 3-D structure for basic perovskite solar cell in (a) validation model (b) Yasodharan et al.	14
Figure 12: Contact parameters	16
Figure 13: Simulation result for V_{oc} , J_{sc} , P_{max} , P_{max} Voltage, fill factor (FF) and power conversion efficiency for validation	17
Figure 14: Current vs. Applied voltage	18
Figure 15: Current density vs. Applied voltage	18
Figure 16: Total charge density vs. Applied voltage.....	18
Figure 17: General structure for (a) perovskite/si tandem solar cell (b) silicon base solar cell in GPVDM	20
Figure 18: 2-dimentional structure for (a) Perovskite/Si tandem solar cell (b) Si base solar cell.....	21
Figure 19: Spiro-OMeTAD chemical structure	21
Figure 20: V_{oc} variation over optical materials	27
Figure 21: J_{sc} variation over optical materials	27
Figure 22: Fill factor variation over optical materials	28
Figure 23: Efficiency variation over optical materials	28
Figure 24: Simulation result for V_{oc} , J_{sc} , P_{max} , P_{max} Voltage, fill factor (FF) and power conversion efficiency for Si base solar cell	30

Figure 25: Charge density vs. Applied voltage	30
Figure 26: Total charge density vs. Applied voltage	30
Figure 27: Current vs. Applied voltage	31
Figure 28: Current density vs. Applied voltage	31
Figure 29: Recombination prefactor vs. Applied voltage.....	31

List of Tables

Table 1: Characteristics of layers	15
Table 2: Electrical parameters used in simulation	15
Table 3: Parasitic Components	16
Table 4: Comparing results of validation	17
Table 5: Simulation parameter comparison	18
Table 6: Characteristics of layers in perovskite/Si tandem solar cell	22
Table 7: Characteristics of layers in silicon base solar cell	22
Table 8: Electrical parameters for perovskite/Si tandem solar cell	23
Table 9: Electrical parameters for silicon base solar cell	24
Table 10: Results for varied front contact materials in perovskite/Si tandem solar cell	26
Table 11: Band gaps of oxides.....	29
Table 12: Simulation information.....	32

Nomenclature and Abbreviations

η	Efficiency
μ	Mobility
μ_{avg}	Average mobility
μ_e	Electron mobility
μ_h	Hole mobility
τ	Recombination time constant
k	Recombination constant
$n(x)$	Density of electrons at any given point in the device
$p(x)$	Density of holes at any given point in the device
R	Recombination rate
Ag	Silver
Al	Aluminium
Al_2O_3	Aluminium oxide
CaTiO_3	Calcium Titanium Oxide
Cr	Chromium
Cu	Copper
Cu_2O	Copper oxide
E_g	Band gap
FF	Fill factor
FTO	Fluorine-doped tin oxide
GaAs	Gallium Arsenide
GPVDM	General-purpose Photovoltaic Device Model
HTL	Hole transport layer
IR	Infra-red
ITO	Indium tin oxide
J_{sc}	Short-circuit current
jv-curve	Current density versus applied voltage curve
LED	Light emitting diode
MoO_x	Molybdenum oxide
n_{free}	Free electrons

NREL	National Renewable Energy Laboratory
OLED	Organic light-emitting diodes
OSC	Organic solar cell
Pb	Lead
PCE	Power conversion efficiency
Pd	Palladium
p^{free}	Free holes
PSC	Perovskite solar cell
PV	Photovoltaic
R_s	Series resistance
R_{shunt}	Shunt resistance
Si	Silicon
SiN	Silicon nitride
SiO ₂	Silicon dioxide
Sn	Tin
SnO ₂	Tin oxide
ssDSSC	Solid-state dye-sensitised solar cells
TiO ₂	Titanium oxide
UV	Ultra-violet
V ₂ O ₅	Vanadium Oxide
VL	Visible light
V_{oc}	Open-circuit voltage
X_i	Electron affinity
Zn	Zinc
ZnO	Zinc oxide

Chapter 1 Introduction

A key challenge of the 21st century is finding energy solutions, in which renewable sources of energy are most popular. Solar power is one such source used globally for various purposes. The solar energy is harnessed by use of solar cells for conversion to electrical energy to be used in households, industry and street lighting.

Although total photovoltaic (PV) energy production is quite small in scale, it is growing in demand and production as the future of fossil fuel based energy seems bleak, considering that fossil fuels cannot be replenished once depleted.

Many different types of solar cells and solar cell materials have undergone production as research found more efficient and feasible materials for use in the cells. The most commonly used materials are Gallium Arsenide (GaAs) and Silicon solar cells, which have proven to be most efficient and feasible for use in commercial applications. However, through research of a newly found mineral called Perovskite, news doors of possibility have opened up to improve the solar photovoltaic (PV) cells further.

Perovskite [1] is a mineral found in the Ural Mountains and named after Lev Perovski, the founder of the Russian Geographical Society. The mineral has a structure known as perovskite structure where the lattice has a form of ABX_3 as shown in figure 1 [1], where the molecular cation (positively charged) A is in the centre of a cube, while the corners are occupied by cations B, and the faces are occupied by anions (negatively charged) X. Figure 1 shows the lattice structure. The two structures in the figure are equivalent; the structure on the left is drawn with A at the centre, while the structure on the right is drawn with B at the centre. True Perovskite is composed of calcium, titanium and oxygen in the form of $CaTiO_3$, but any compound having the same lattice structure can be called a perovskite mineral.

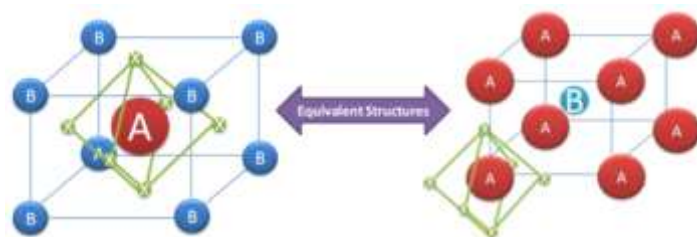


Figure 1: A generic perovskite crystal structure of the form ABX_3

The properties, such as superconductivity, giant magnetoresistance, spin-dependent transport and catalytic properties, of perovskite can be changed by altering the atoms/molecules in the structure.

The reason for the rise of attention for Perovskite solar cells can be demonstrated via graphs shown in figures 2 [1] and figure 3 [2]. Figure 2 shows the comparison of power conversion efficiencies of perovskite-based devices to emergent PV research technology and traditional thin-film PVs, over the last decade. The graph shows how fast the efficiency has improved compared to most other technologies over a relatively short period of time.

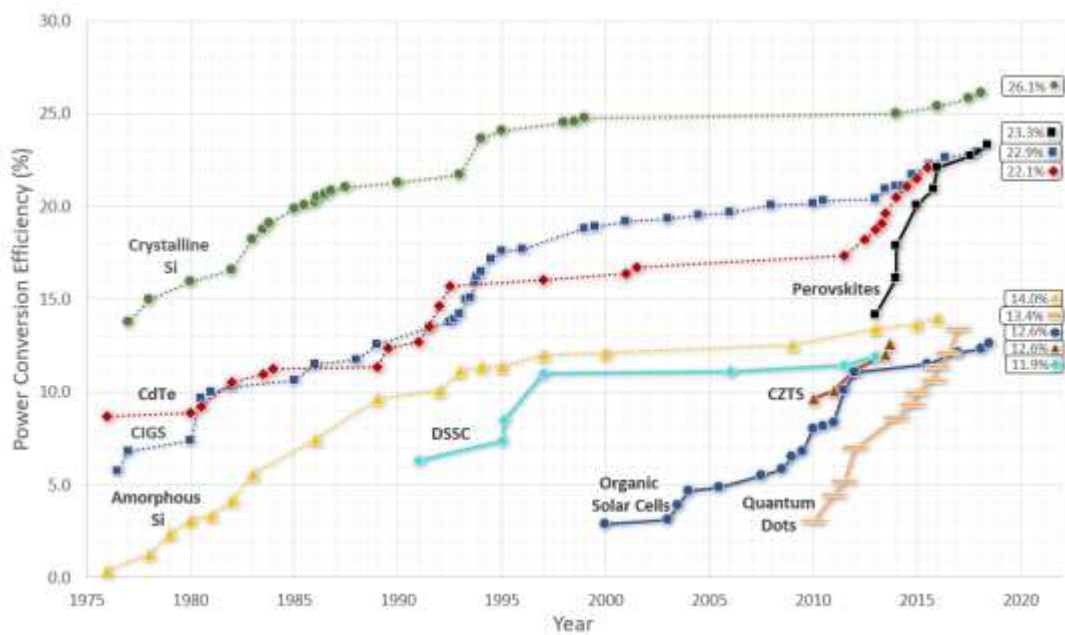


Figure 2: Power Conversion Efficiency by Year for various cell materials

Figure 3 shows the open-circuit voltage compared to the band gap for a competitors of perovskites. It demonstrates the amount of photon energy lost in the light energy to electrical energy conversion process. Standard organic solar cells have a loss as high as 50% of the absorbed photon energy, whilst perovskite solar cells consistently exceed 70% photon energy utilisation and have the potential to become cheaper than crystalline silicon solar cells which are already 1000 times cheaper than GaAs solar cells. The maximum photon energy utilisation is defined as the open circuit voltage V_{oc} divided by the optical Band gap (E_g) for common single junction solar cells

material systems [1]. It is calculated from state of the art cells detailed in NREL efficiency tables.

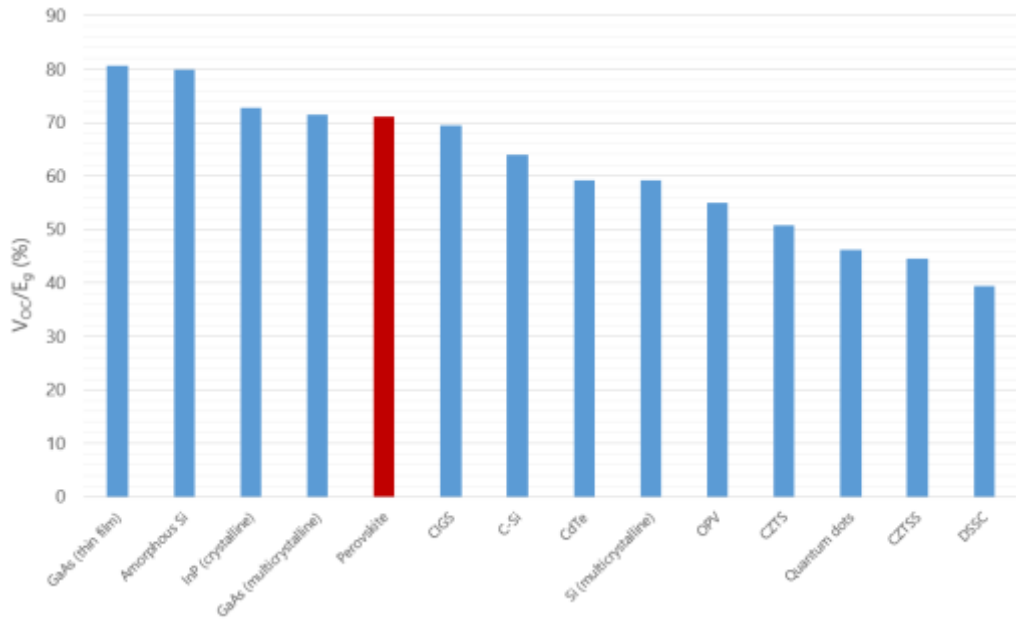


Figure 3: Open-circuit Voltage for cell materials

Although the commercialisation of perovskite solar cells still faces obstacles in the fields of fabrication and stability, their use in perovskite/Si tandem solar cells has rapidly advanced with above 25% efficiency achieved in most cases. Apart from solar cells, perovskites also have significant potential in light emitting diode (LED) and resistive memory applications.

Perovskites have been around for more than a decade, but only very recently have been considered by researchers to be practical. Recent studies showed cells made of perovskite to have efficiency higher than 23% [1,3]. Perovskite cells in tandem application [4] has also been planned by several big names in the market with quite a generous funding [5] after perovskite's initial stability concerns were addressed [6].

1.1 Solar Cells

Solar cells, or PV cells, are devices which directly convert photon energy (light energy) to electrical energy through photovoltaic effect. Solar cells are usually made

from silicon or GaAs. As the materials range from amorphous (noncrystalline) to polycrystalline to crystalline silicon forms, the efficiency increases and costs decrease. Figure 4 [7] shows the structure of a solar cell.

Batteries or fuel cells utilise chemical reactions, and generators utilise moving parts to produce electric power, however solar cells do not require such parts and can directly perform the conversion within the cell material.

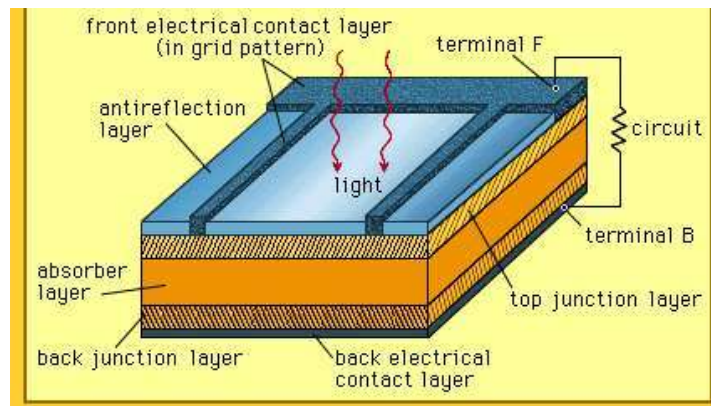


Figure 4: Diagram of a solar cell structure

Solar cells in the form of solar panels are installed by homeowners on rooftops as a more eco-friendly replacement for conventional electric supply. They are installed in toys, calculators and radios alongside batteries, and have been increasingly used in many similar small scale applications. Solar panels also play a key role in applications where electric power needs to be supplied to remote terrestrial locations where conventional sources of power are unavailable or expensive to install. Together with their ability to operate in the absence of fuel, solar panels are a popular power source for most space installations (communications and weather satellites, space stations, rovers). However, they are ineffective in case of probes or satellites sent into interstellar space due to their distance from the Sun.



Figure 5: Solar panels installed on Satellite (Photo: NASA)



Figure 6: Rooftop solar panel in Bangladesh (Photo: Zahiduddin Saimon, Bangladeshpost.net)

1.2 Solar Cell Structure and Operation

Open-circuit voltage (V_{oc}) is the maximum voltage the solar cell can produce when illuminated [8]. Short-circuit current (J_{sc}) is the maximum current the cell can produce when it is illuminated [8]. Efficiency (η) of a cell is the maximum current the cell can produce when it is illuminated [8]. Figure 7 [8] shows the above mentioned terms on a general current density against applied voltage (jv) curve.

Light enters the device through an antireflection layer to the energy-conversion layers beneath it, to minimise the losses due to reflection. The energy-conversion layers typically consist of the front contact, absorber or active layer, and the back contact. Solar cells can have other layers within the absorber section including buffer layers. The contact layers carry the electric current out to an external load. The front contact is usually present in a grid pattern. Both contact layers are good conductors. The back contact is always made of metal.

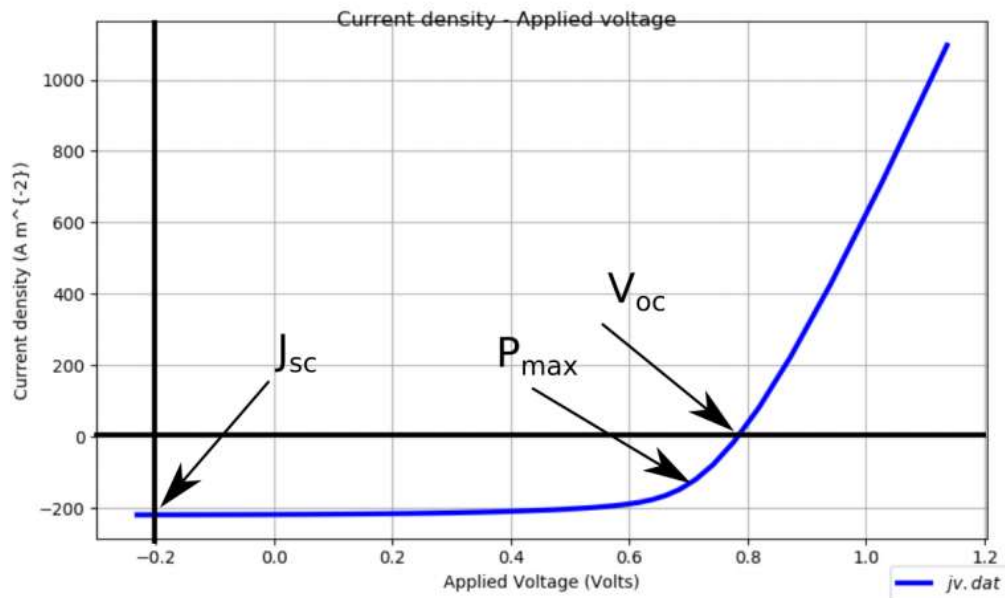


Figure 7: V_{oc} , J_{sc} , P_{max} on jv curve

Solar cells perform mainly due to the interaction of photons with the active layer of the cell. The active layer is the layer of material which converts photons into electrons and holes. For an organic solar cell, a thickness of 50 nm is considered very thin, while 400 nm is considered very thick for efficient device operation.

The light from the sun consists of wavelengths within the spectrum of ultraviolet (UV) to visible light (VL) or infra-red (IR). Only the wavelengths in the VL range can be seen by the human eye. Within the solar cells, some parts are designed to absorb light, whilst some layers are designed to conduct charge carriers out of the cell.

The absorption of VL is best performed by semiconductors. This material as the absorber occupies most of the space in a solar cell. When light is incident on the solar cell, electrons in the absorber layer are excited from a lower energy “ground state” to a higher energy “excited state”. This transitions the electrons from being bound to the atoms in the solid, to being free to move through the solid. The absence of the electrons in their original location forms holes. The electrons and holes, thus become the charge carriers for the device.

To direct the flow of current via the charge carriers, contact layers are added which induce a built-in electric field producing the photovoltaic effect.

A very thin device is unable to absorb enough photons so cannot achieve greater efficiency. Theoretically, a very thick device is able to absorb all the photons incident on it from the sun to achieve greater efficiency. However, the thicker the device, the further the electrons and holes will have to travel from point of generation to the contact layers where they exit the device to perform useful work in the external circuit. This will prolong the stay of the electrons or holes in the device post photogeneration making it more probable for an electron to meet a hole, or vice versa, causing them to annihilate each other's opposite charges and be instantaneously destroyed. This phenomenon is known as recombination. Recombination lowers the efficiency as the electron or hole worth of some amounts of photon energy is wasted in the process.

The recombination rate (R) [8] is given by,

$$R(x) = kn(x)p(x)$$

Where,

$n(x)$ is the density of electrons at any given point in the device

$p(x)$ is the density of holes at any given point in the device

k is the recombination constant

The recombination constant determines the efficiency of the recombination process. If k is equal to zero, then there is no recombination. In GPVDM software, this is denoted by the n_{free} to p_{free} recombination constant which is usually set to $1e-20$.

To avoid recombination, charge carriers must spend as little time as possible in the device, and should move towards the contacts to enter the external circuit swiftly. The speed at which electrons and holes move within a device is determined by the electron and hole charge carrier mobility.

Mobility (μ) is the time taken by a charge carrier to exit the device after being generated. The average mobility [8] for a device is given by,

$$\mu_{avg} = \frac{\mu_e + \mu_h}{2}$$

Where,

μ_{avg} is the average mobility

μ_e is the electron mobility

μ_h is the hole mobility

Tau (τ) denotes the recombination time constant, which is the average time a charge carrier will survive without recombining. The product of mobility and recombination time constant ($\mu \cdot \tau$) gives the measure of how efficient the solar cell is. A large value indicates better efficiency. This is illustrated in figure 8 [8].

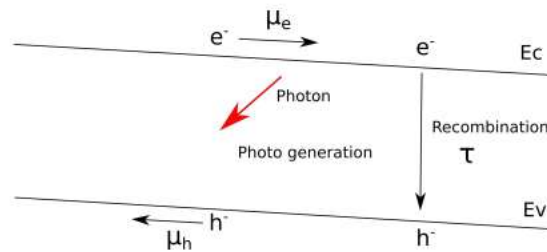


Figure 8: Charge carriers under the influence of μ and τ

A solar cell acts like a diode, but are not perfect diodes. In reality, they have both series resistance (R_s) and shunt resistance (R_{shunt}). Due to the flat broad contacts on the solar cell, there is often a capacitance associated with the device. The series resistance accounts for the resistance of the contacts. Shunt resistance includes the impurities in the active layer responsible for forming short circuits between the front and back contacts. If R_{shunt} equals zero, i.e. full short circuit, the solar cell would not work. If R_{shunt} is very big (say 1 $M\Omega$), the solar cell would work better.

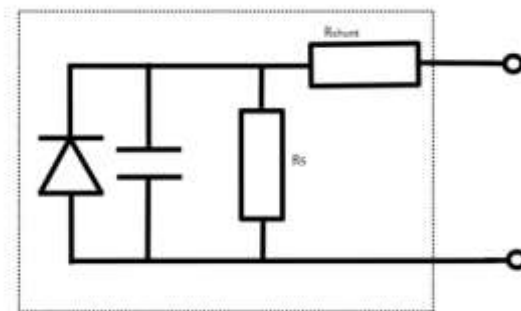


Figure 9: Parasitic components of a solar cell

1.3 Tandem Solar Cells

One method of increasing the efficiency of solar cells is by splitting the spectrum and using a solar cell that is optimised to each section of the spectrum. This can be achieved through a tandem solar cell. Such cells can be individual cells or connected in series.

By adding more devices in series to form a tandem cell, it allows for each device to be optimised to a narrower spectrum, giving a higher overall efficiency. These are simpler to fabricate. The band gaps within the device, however, are constrained due to the same current flowing through each cell. The most common preparation for tandem cells is to grow them monolithically. This arrangement ensures that all the cells are grown as layers on the substrate, such that the tunnel junctions connect the individual cells.

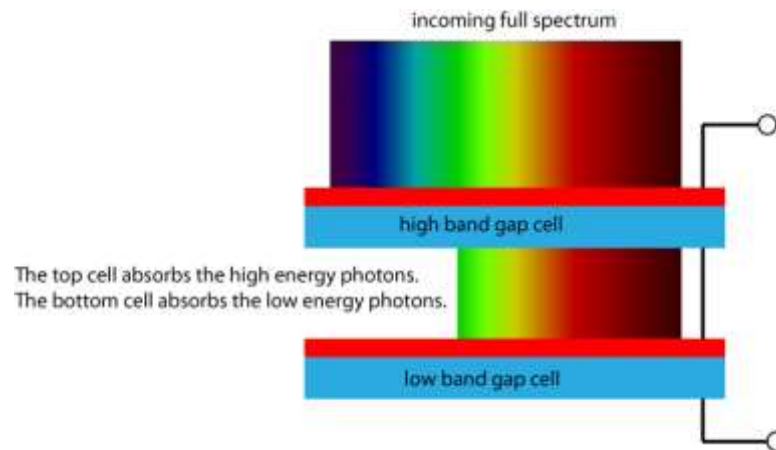


Figure 10: Series connected tandem solar cell

This thesis studies a solar cell consisting of perovskite layer above silicon layer [9] in the form of a perovskite/Si tandem solar cell. Perovskite/Si tandem cells have undergone research and advances in both stability and compatibility [10–12], thus is a good choice for further research.

Chapter 2 Literature Review

Many research has been conducted on the context of perovskite/silicon tandem solar cells and the effect of various contact materials.

The review by Jošt, et al., 2020 [13], outlines some challenges for further development related to the front contact materials in perovskite/silicon solar cells. Through their review they conclude that the key challenges include transparency, sputter damage to perovskite and contact layers, conformality, and protective buffer layer. It outlines the following researches conducted to solve these challenges.

In 2015, Mailoa, et al., first invented a perovskite/silicon tandem cell on an n-type Si homojunction bottom cell with standard diffused junctions [14]. Spiro-OMeTAD was used as the front contact along with a mechanically transferred mesh of silver nanowires. This resulted in the cell being strongly limited by a low V_{oc} of 1.58 V, a low J_{sc} of 11.5 mA cm^{-2} , and a fill factor (FF) of 75%. The limited J_{sc} resulted from the thick, doped Spiro film which lead to an overall parasitic absorption equivalent to a loss in photogeneration current density of around 8.4 mA cm^{-2} . The cell had an efficiency of 13.7%.

In 2016, Werner, et al., prepared a cell with the same Spiro as Mailoa's cell, but with a transparent front contact formed with evaporated molybdenum oxide (MoO_x) as a buffer layer and a sputtered IO:H/ITO top electrode [15]. This led to the efficiency rising to 16.4%.

In 2017, Wu, et al., further improved the efficiency to 22.5% by keeping the front contact same, but changing the bottom cell to passivating Al_2O_3 and SiN_x films with local contact openings and Cr/Pd/Ag point contacts covered on the front with an ITO blanket layer [16].

In 2018, Zheng, et al., came up with larger devices with an efficiency of 21.0% with the same front contact, but with an interconnecting layer of SnO_2 processed by spin coating from a colloidal precursor and annealing at $150 \text{ }^\circ\text{C}$ [17]. Zheng and his team made a cell of 21.8% steady-state efficiency, later in the same year [18].

From the above mentioned researches, it can be seen that changing the contact materials or their preparation in conjunction with other materials significantly affects the solar cell efficiencies. The efficiency of solar cell also depends on the work function [9, 15] of the front and back contacts. Good contact layers should provide low nonradiative interface recombination losses at V_{oc} , but strong luminescence quenching [20]. Several studies reviewed also showed that Spiro trapped a lot of light causing loss of photon energy, thus there is a necessity to develop a more transparent front contact [17, 18].

In the paper by Ellimer, et al., 1996 [23], a method of sputtered ZnO/ZnO:Al contact layer production was studied. In their research, they concluded that the process was possible to create films which showed better performances as opposed to simple ZnO:Al films.

A work on the influence of contact layers on PV performance of silicon solar cell by Ali, et al., 2017 [24], studied a p-n homojunction Si solar cell with Fluorine-doped tin oxide (FTO) as front contact and Zinc (Zn) as back contact. The simulations were run on AMPS-1D (analysis of microelectronic and photonic structures one dimensional). They concluded that with the chosen contact materials, an efficiency of 29.275% could be achieved from the device. They also suggested that the efficiency could be further improved by controlling the Band gap.

Ahmed, et al., 2019, used GPVDM to simulate the operation and functionality of a working Sn perovskite/Cu₂O HTL/Cu back contact device against a standard Pb perovskite/Spiro HTL/Ag back contact device [25]. Their results showed a 22.9% efficiency for the former mentioned device and a 24.6% efficiency for the latter, at the same active layer thickness. They concluded that the Sn perovskite/Cu₂O HTL/Cu back contact device has a higher HTL hole mobility, combined with greater interfacial electron affinity differential, and that its improved performance is due to the reduction of defect density/recombination centres both within each layer matrix and in the interfacial contacts [25].

Afrasiab, et al., 2020, simulated their work on SCAPS version 3.3.0.7 to investigate the prospective efficiencies of perovskite/Si tandem solar cell as compared with silicon based solar cell and perovskite based solar cell [26]. The results concluded that

their proposed tandem solar cell model demonstrated high efficiency compared to the other mentioned devices. They concluded it is due to the improved ability of broadband absorption of incoming photons. The refined tandem cell had an efficiency of 28.50%.

Researches related to simulation using GPVDM include optimising the power conversion efficiency of perovskite solar cell [27]. In their research, Aitezaz, et al. 2020, concluded that there is a direct relation between the optimum layer thickness and output power conversion efficiency (PCE), thus establishing that greater thickness aids more photon absorption resulting in higher electron-hole pairs. They also concluded that the optimum band gap plays an essential role in the PCE, where in their research the PCE jumped from 13.2% to 25.59%. However, they found no effect of shunt and series resistances on the PCE.

In the paper on thin-film tandem organic solar cells, Farooq, et al., 2020, compared three different types of organic tandem cells for their performance using GPVDM. They concluded that the homo tandem cell based on P3HT: PCBM material supports slightly low efficiency compared to PTB7: PCBM based cell, because of its small absorption coefficient [28]. However, the optimized hybrid tandem solar cell showed high efficiency, which they concluded happened because the top active layer absorbed higher frequency photons than the bottom layer.

Another work using GPVDM includes the research by Sittirak, et al., 2019, where they studied the effect of layer thickness and charge mobilities on some parameters in perovskite solar cell based on structure of FTO/TiO_x/SnO₂/FAIMABrPbI₂PbBr₂/Spiro-OMeTAD/Ag [29]. They obtained an efficiency of 23.88%, and electron and hole mobilities of 2e-5 m²V⁻¹s⁻¹ and 2e-6 m²V⁻¹s⁻¹, respectively, for their optimised model.

Hima, et al., 2019, also worked on the optimisation of a perovskite solar cell for high PCE [30] using ATLAS device simulation software. They varied the layer thickness for the study and found that the perovskite layer thickness of both CH₃NH₃PbI₃-based solar cell and CH₃NH₃SnI₃-based solar cell has an effect on electrical parameters in comparison with that of hole and electron transporting layers, where CH₃NH₃PbI₃ has better electrical performance.

Chapter 3 Methodology

3.1 GPVDM

GPVDM (General-purpose Photovoltaic Device Model) is an open source one-dimensional or two-dimensional opto-electronic device model used to simulate solar cells, LEDs, diodes, and so on. It simulates through solving drift diffusion equations using the finite difference method, and optical equations using ray tracing or transfer matrix method. Developed by Dr. Roderick C. I. MacKenzie, it was released to the public to ensure more research to be done on Perovskites.

The charge transport is simulated on the basis of the following equations:

- Gauss's Law

$$\nabla \epsilon_o \epsilon_r \cdot \nabla \phi = q \cdot (n - p)$$

- Electron driving terms

$$J_n = q \mu_n n \nabla E_c + q D_n \nabla n$$

- Hole driving terms

$$J_p = q \mu_p p \nabla E_v - q D_p \nabla p$$

- Electron continuity

$$\nabla \cdot J_n = q \left(R_n + T_n + \frac{\partial n_{free}}{\partial t} \right)$$

- Hole continuity

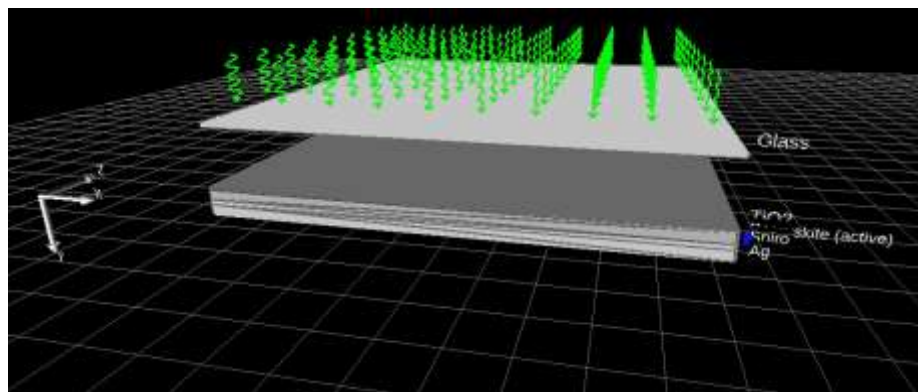
$$\nabla \cdot J_p = -q \left(R_p + T_p + \frac{\partial p_{free}}{\partial t} \right)$$

In GPVDM, layers are categorized into three types – active, other and contact. The electrical model is solved over the active layers, thus they have a separate set of

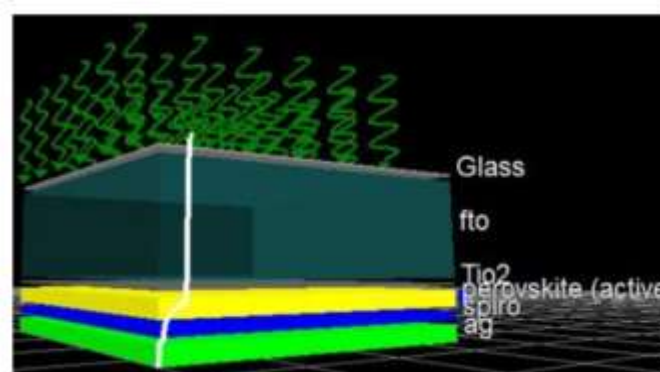
electrical parameters which can be edited as per requirement. The contact layers are used to define the electrical contacts, but no electrical equations are solved over them. No electrical equations are solved over the other layers.

3.2 Validation

A validation for GPVDM based research was performed with reference to the paper on the “Effect of Layer Thickness on Power Conversion Efficiency in Perovskite Solar Cell: A Numerical Simulation Approach” [31]. The purpose of the validation is to confirm that the results from the validation performed using the information available in the paper will follow trend of the results in the paper, through qualitative analysis.



(a)



(b)

Figure 11: 3-D structure for basic perovskite solar cell in (a) validation model (b) Yasodharan et al.

Table 1: Characteristics of layers

Layer Name	Thickness	Optical Material	Layer Type
Glass	2.5e-08	Glasses/glass	Other
FTO	1.2e-06	Oxides/fto	Contact
TiO2	2.5e-08	Oxides/tiox	Other
Perovskite	2.0e-07	Perovskites/std_perovskite	Active layer
Spiro	1.0e-07	Small_molecules/spiromeotad	Other
Ag	2.0e-07	Metal/ag	Contact

Table 2: Electrical parameters used in simulation

Electron trap density	8.667213e+24	$\text{m}^{-3}\text{eV}^{-1}$
Hole trap density	1.798229e+24	$\text{m}^{-3}\text{eV}^{-1}$
Electron tail slope	42e-3	eV
Hole tail slope	41e-3	eV
Electron mobility	1e-4	$\text{m}^2\text{V}^{-1}\text{s}^{-1}$
Hole mobility	1e-4	$\text{m}^2\text{V}^{-1}\text{s}^{-1}$
Relative permittivity	3	Au
Number of traps	5	Bands
Free electron to trapped electron	3.334112e-21	m^{-2}
Trapped electron to free hole	5.988991e-19	m^{-2}
Trapped hole to free electron	2.778942e-21	m^{-2}
Free hole to trapped hole	6.42594e-20	m^{-2}
Effective density of free electron states (@300K)	5e+26	m^{-3}
Effective density of free hole states (@300K)	5e+26	m^{-3}
Xi	3.598	eV
Eg	1.099	eV
n_{free} to p_{free} Recombination rate constant	1e-21	m^3s^{-1}
Free carrier statistics	Maxwell Boltzmann - analytic	type

Table 3: Parasitic Components

Shunt resistance	1.2	Ohms m ²
Series resistance	1.001859e+00	Ohms
Other layers	0.0	m

Figure 11 shows the structure designed in GPVDM following the layer structure mentioned in Yasodharan et al. Table 1 shows the subsequent layers which were added to the structure and their respective parameters. Table 2 includes the electrical parameters for the active layer, as seen in the GPVDM electrical parameter editor.

Table 3 highlights the parasitic component parameters, while the contact details are provided in figure 12, however these two information were not provided by Yasodharan et al. It is also to be noted that the information in table 2 includes more details to electrical parameters which were not defined in the paper, thus were assumed as is mentioned by the built-in figures within GPVDM.

Name	Top/Bottom	Applied voltage	Charge density/ Fermi-offset	Majority carrier	Physical model	
top	top	Ground	0	1e25 m ⁻³ / 0.10 eV	Electron	Ohmic
	bottom	Change	Vsig	1e25 m ⁻³ / 0.10 eV	Hole	Ohmic

Figure 12: Contact parameters

A simulation was run to verify the short circuit current (J_{sc}), open circuit voltage (V_{oc}) and conversion efficiency as found in the reference, for a perovskite layer thickness of $2.0e-07$ m.

The results from the simulation are highlighted in figure 13. Table 4 shows how the results from the reference paper compare to the results from the validation. According to this table, the error in V_{oc} is within acceptable range (taking acceptable range as below 10%), however there is very high error in J_{sc} and conversion efficiency.

The high errors in J_{sc} and conversion efficiency can be explained due to the following reasons.

- All the parameters for the simulation were not mentioned in the reference paper, thus some parameters had to be assumed or the built-in parameters had to be used, for instance the parasitic component and contact parameters.
- A lot of the solar cell performance depends on the defined doping levels for the active layers. This was not mentioned in the reference paper, so the given levels as per the software were used.
- GPVDM is updated regularly. The reference paper was published in 2019, while the software for this thesis was downloaded in 2020. The versions have changed with more improved interface and updated database. A new version is already available for download on their website. This may have caused the built-in values to be different which affected the results.
- The information regarding the electric properties of thin films and their interfaces are necessary to fully understand how a solar cell based device functions. The perovskite absorbers, carrier recombination lifetimes, which are governed by the density distribution of defect states in the band gap, determine cell V_{oc} and fill factor [13], which can be located in the film's bulk. Transport properties for electrons and holes are important parameters for the fill factor and for carrier selective contact materials.

```
Voc= 0.413536 (V)
Jsc= -116.794786 (A/m^2)
Pmax= 35.718033 (W/m^2)
Pmax Voltage= 0.338732 (V)
FF= 73.952209
Efficiency= 3.571803 percent
```

Figure 13: Simulation result for V_{oc} , J_{sc} , P_{max} , P_{max} Voltage, fill factor (FF) and power conversion efficiency for validation

Table 4: Comparing results of validation

Parameters	Data from Paper	Validated data	Error in data
V_{oc} (V)	0.45	0.413536	8.10
J_{sc} ($A m^{-2}$)	398	116.7948	70.65
Conversion Efficiency (%)	14.5	3.571803	75.36

Even so, the results imply that the validation is not completely deviated as at least one parameter matched. Moreover, the graphical outputs can be seen to have similar trends as that seen in the reference paper.

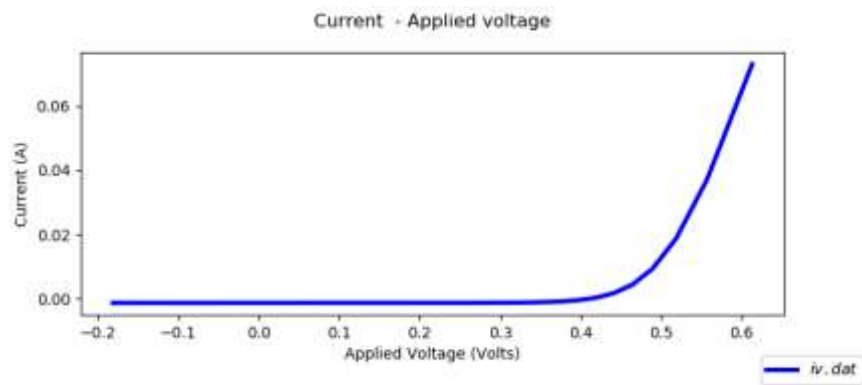


Figure 14: Current vs. Applied voltage

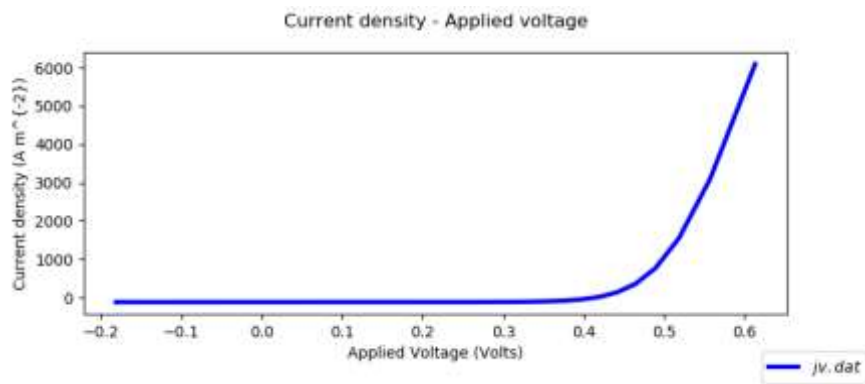


Figure 15: Current density vs. Applied voltage

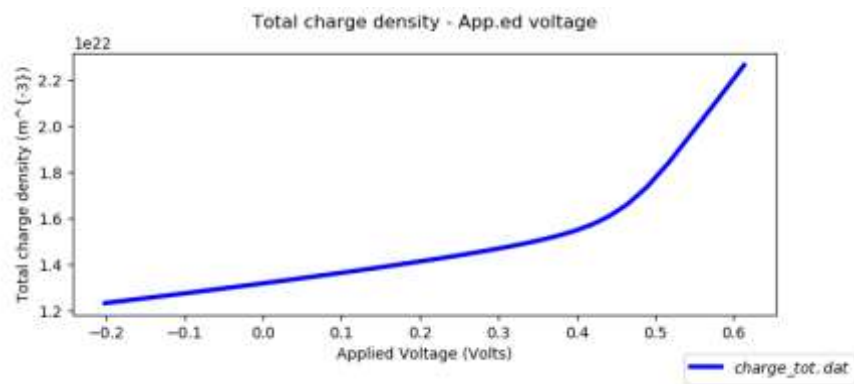


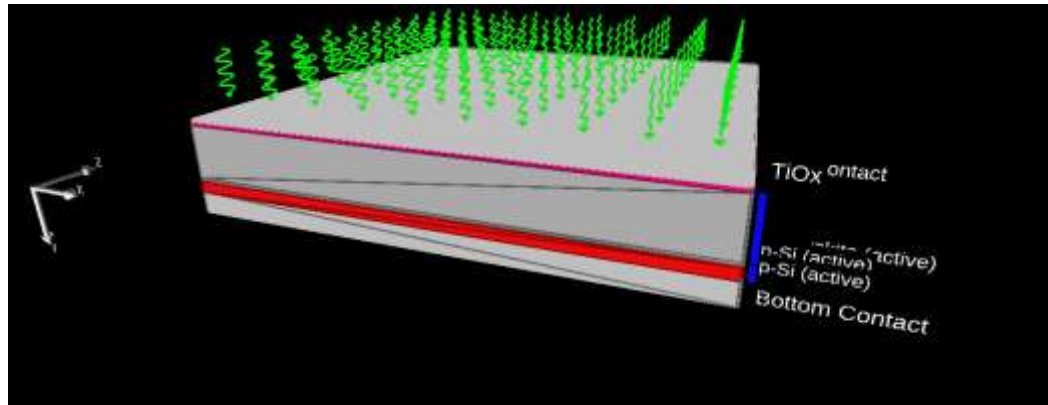
Figure 16: Total charge density vs. Applied voltage

Table 5: Simulation parameter comparison

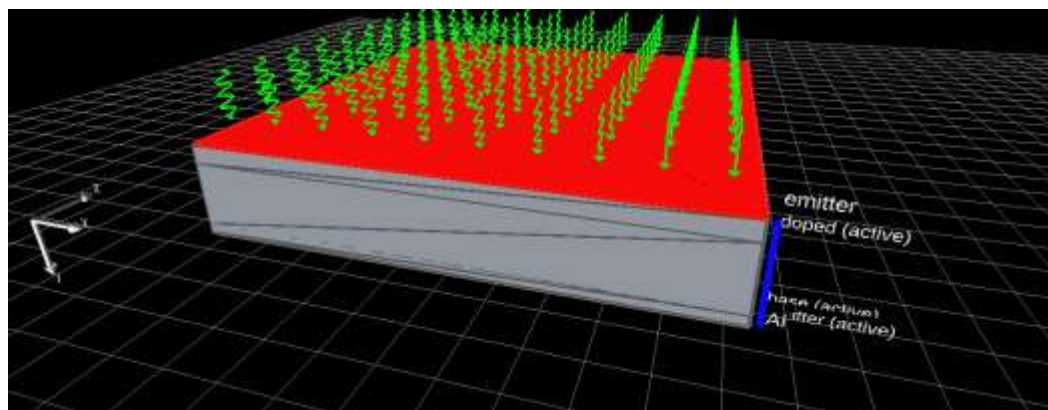
Parameters	Reference paper	Validated data	Percentage Error	Unit
Fill factor	0.743351	0.739522	0.52	a.u.
Power conversion efficiency	9.017149	3.571803	60.39	Percent
Max power	90.171487	35.718033	60.39	Wm ⁻²
V _{oc}	0.453533	0.413536	8.82	V
Recombination time constant at V _{oc}	5.291787e-07	1.123100e-06	112.23	s
Recombination rate at V _{oc}	9.330719e+27	3.342884e+27	64.17	m ⁻³ s ⁻¹
Average carrier density at P _{max}	2.908195e+21	2.534512e+21	12.85	m ⁻³
Recombination time constant	3.371245e-6	8.297898e-06	146.14	m ⁻¹
Trapped electrons at V _{oc}	5.010042e+20	1.034645e+21	106.51	m ⁻³
Trapped holes at V _{oc}	1.783519e+20	1.758967e+20	1.38	m ⁻³
Free electrons at V _{oc}	8.243883e+21	2.112233e+22	156.22	m ⁻³
Free holes at V _{oc}	8.522118e+21	9.179960e+21	7.72	m ⁻³
J _{sc}	-2.674646e+02	-1.167948e+02	56.33	Am ⁻²
Total carriers (n+p)/2 at V _{oc}	1.662688e+22	3.627347e+22	118.16	m ⁻³
Current density at max power	-	-1.054462e+02	-	Am ⁻²
Voltage at max power	-	3.387323e-01	-	V

From qualitative analysis, it can be stated that the result has been validated.

3.3 Modelling



(a)



(b)

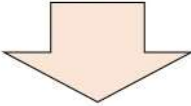
Figure 17: General structure for (a) perovskite/si tandem solar cell (b) silicon base solar cell in GPVDM

Figure 17 (a) shows the general structure for the perovskite/Si tandem solar cell, while figure 17 (b) shows the general structure for the silicon base solar cell. The structures show the layers included in the models along with the chosen set of thickness which was held constant during the simulation. Additionally, figure 18 (a) and (b) show how the structures look like in the GPVDM interface. The green arrows indicate incoming sunlight which are also shown in the previously mentioned figures.

As shown in the figures, the purpose of the work is to vary the front and back contact materials, keeping all other parameters constant. An initial simulation using Fluorine-doped Tin Oxide (FTO) as front contact and Silver (Ag) as back contact was

performed for both the cells. The rest of the simulations for varying contact materials was run for the tandem solar cell. The back contact material was held constant with Ag. The front contact materials chosen for the study were FTO, Indium Tin Oxide (ITO), Silicon dioxide (SiO₂), Titanium oxides (TiO_x), Vanadium Oxide (V₂O₅), Zinc Oxide (ZnO), Ag, and Aluminium (Al).

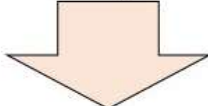
Sunlight



Glass	2.5e-10
Front Contact	1.0e-08
TiOx	2.5e-08
Perovskite	5.0e-07
Spiro	2.0e-08
n-Si	2.0e-08
p-Si	1.0e-07
Back Contact	2.0e-07

(a)

Sunlight



Glass	2.5e-10
Front Contact (emitter)	1.0e-08
Si (doped)	2.0e-06
Si (base)	7.0e-06
Si (emitter)	1.0e-06
Back Contact (emitter)	2.0e-07

(b)

Figure 18: 2-dimensional structure for (a) Perovskite/Si tandem solar cell (b) Si base solar cell

Table 6 and table 7 show the layer parameters used for the simulations. The FTO in the front contact was used to run the initial simulation and later varied for study. Table 8 summarises the electrical parameters for the active layers in the tandem solar cell. Table 9 summarises the electrical parameters for the active layers in the silicon base solar cell.

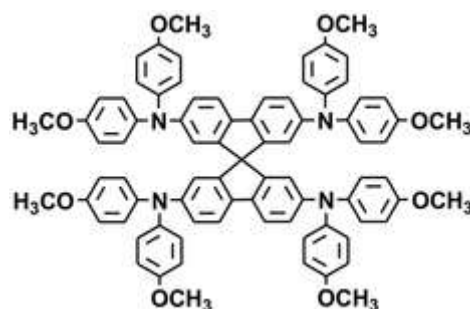


Figure 19: Spiro-OMeTAD chemical structure

Here, glass is taken as a protective material to prevent the solar cell being exposed to environment directly (water, moisture, dust, and etcetera). TiO_x is taken as a window layer. This layer will reduce front surface recombination. Perovskite and silicon will act as active layers as mentioned in the table. Spiro-OMeTAD (mentioned as Spiro in the table) will act as an absorber layer. Spiro-OMeTAD (figure 16 [32]) is one of the most studied and suitable hole transport layer materials due to the simplicity of its implementation and high performance in electronic devices. The molecule provides high glass transition temperature, morphological stability and easy processability while maintaining good electronic properties [32]. Spiro-MeOTAD has been widely used in solid-state dye-sensitised solar cells (ssDSSC), organic light-emitting diodes (OLED), perovskite solar cells (PSCs) and polymer based organic solar cells (OSCs).

Table 6: Characteristics of layers in perovskite/Si tandem solar cell

Layer Name	Thickness	Optical Material	Layer Type
Glass	2.5e-10	Glasses/glass	Other
Front Contact	1.0e-08	Oxides/fto	Contact
TiO _x	2.5e-08	Oxides/tiox	Other
Perovskite	5.0e-07	Perovskites/std_perovskite	Active layer
Spiro	2.0e-08	Small_molecules/spiromeotad	Other
n-Si	2.0e-08	Inorganic/si	Active layer
p-Si	1.0e-07	Inorganic/si	Active layer
Back Contact	2.0e-07	Metal/ag	Contact

Table 7: Characteristics of layers in silicon base solar cell

Layer Name	Thickness	Optical Material	Layer Type
Glass	2.5e-10	Glasses/glass	Other
Emitter	1.0e-08	Oxides/fto	Contact
Doped	2.0e-06	Inorganic/si	Active layer
Base	7.0e-06	Inorganic/si	Active layer
Emitter	1.0e-06	Inorganic/si	Active layer
Ag	2.0e-07	Metal/ag	Contact

Table 8: Electrical parameters for perovskite/Si tandem solar cell

PARAMETER	VALUE			UNIT
	Perovskite	n-Si	p-Si	
Electron trap density	1e+20	1e+25	1e+25	$m^{-3}eV^{-1}$
Hole trap density	1e+20	1e+25	1e+25	$m^{-3}eV^{-1}$
Electron tail slope	30e-3	60e-3	60e-3	eV
Hole tail slope	30e-3	60e-3	60e-3	eV
Electron mobility	20e-4	1e-4	1e-4	$m^2V^{-1}s^{-1}$
Hole mobility	20e-4	1e-4	1e-4	$m^2V^{-1}s^{-1}$
Relative permittivity	20	6	6	Au
Number of traps	5	4	4	Bands
Free electron to trapped electron	1e-21	1e-20	1e-20	m^{-2}
Trapped electron to free hole	1e-21	1e-18	1e-18	m^{-2}
Trapped hole to free electron	1e-21	1e-18	1e-18	m^{-2}
Free hole to trapped hole	1e-21	1e-28	1e-28	m^{-2}
Effective density of free electron states (@300K)	5e+26	5e+26	5e+26	m^{-3}
Effective density of free hole states (@300K)	5e+26	5e+26	5e+26	m^{-3}
χ_i	3.75	2	2	eV
E_g	1.6	2	2	eV
n_{free} to p_{free} Recombination rate constant	1e-21	0	0	m^3s^{-1}
Free carrier statistics	Maxwell Boltzmann - analytic	Maxwell Boltzmann - analytic	Maxwell Boltzmann - analytic	type

Table 9: Electrical parameters for silicon base solar cell

PARAMETER	VALUE			UNIT
	Doped	Base	Emitter	
Electron trap density	1e+25	1e+25	1e+20	$m^{-3}eV^{-1}$
Hole trap density	1e+25	1e+25	1e+20	$m^{-3}eV^{-1}$
Electron tail slope	30e-3	30e-3	30e-3	eV
Hole tail slope	30e-3	30e-3	30e-3	eV
Electron mobility	5000e+4	5000e+4	5000e+4	$m^2V^{-1}s^{-1}$
Hole mobility	450e+4	450e+4	450e+4	$m^2V^{-1}s^{-1}$
Relative permittivity	11	11	11	Au
Number of traps	0	0	0	Bands
Free electron to trapped electron	1e-25	1e-20	1e-20	m^{-2}
Trapped electron to free hole	1e-25	1e-20	1e-20	m^{-2}
Trapped hole to free electron	1e-25	1e-20	1e-20	m^{-2}
Free hole to trapped hole	1e-25	1e-20	1e-20	m^{-2}
Effective density of free electron states (@300K)	5e+26	5e+26	5e+26	m^{-3}
Effective density of free hole states (@300K)	5e+26	5e+26	5e+26	m^{-3}
X_i	4.05	4.05	4.05	eV
E_g	1.6	1.6	1.6	eV
n_{free} to p_{free} Recombination rate constant	1e-25	1e-25	1e-25	m^3s^{-1}
Free carrier statistics	Maxwell Boltzmann - analytic	Maxwell Boltzmann - analytic	Maxwell Boltzmann - analytic	type

The contact parameters and parasitic component parameters were taken same as that used in validation. The electrical parameters used are built-in values of GPVDM. The thicknesses for the layers were selected from the built-in values of GPVDM. Additionally, thickness of glass was selected by trial and error to achieve most efficiency. All simulations were run for light intensity of 1.0 suns.

Chapter 4 Result Analysis

Table 10 summarises the results obtained for varying the front contact material in the modelled perovskite/Si tandem solar cell. The graphs in figures 20 to 23 show the comparison for the results obtained in table 11. The results for V_{oc} , J_{sc} , FF and efficiency were obtained directly from coded results within GPVDM. The graphs were generated in MS Excel post simulation.

They show that the maximum V_{oc} and efficiency were both obtained for SiO_2 as front contact material. The maximum J_{sc} was obtained for Ag and Al. Maximum FF was obtained for ITO.

All results were obtained under assumed conditions and values due to lack of suitable data for simulation. As mentioned earlier in this work, the software itself has inadequacies which prevent the results from being close to the accurate values. It is, thus to be noted that the efficiencies obtained in this study are of qualitative value instead of quantitative. The values maybe compared against each other, but not with actual data from experimentation.

Table 10: Results for varied front contact materials in perovskite/Si tandem solar cell

Optical material	V_{oc} (V)	J_{sc} (Am^{-2})	FF	Efficiency (%)
FTO	0.982768	-163.722696	68.474787	11.017688
ITO	0.983248	-167.627528	68.477234	11.286384
SiO_2	0.984093	-174.494032	68.476243	11.758627
TiO_x	0.983248	-167.627528	68.477234	11.286384
V_2O_5	0.978735	-136.450868	68.447638	09.141130
ZnO	0.983944	-173.279853	68.476737	11.675120
Ag	0.934448	-26.375967	67.323621	01.659323
Al	0.934448	-26.375967	67.323621	01.659323

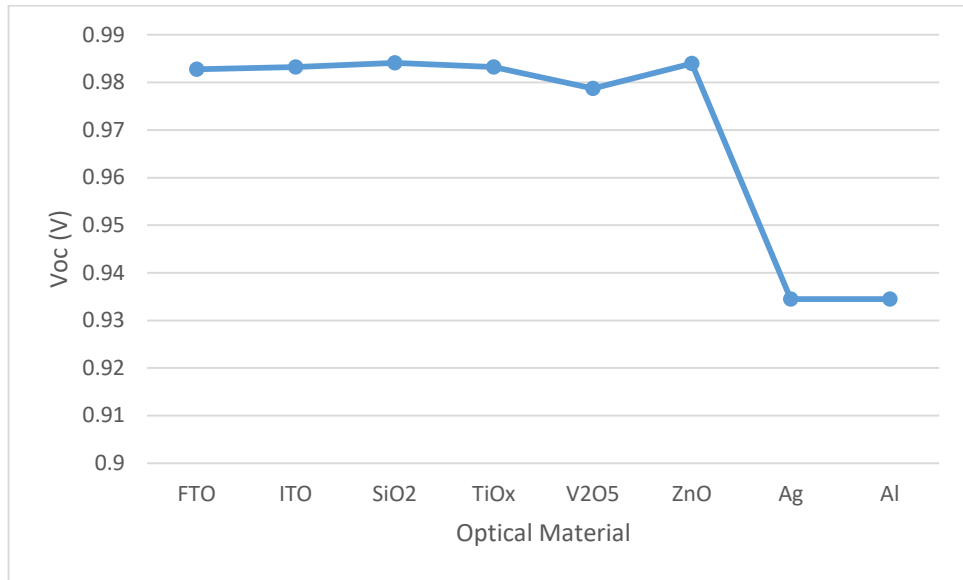


Figure 20: V_{oc} variation over optical materials

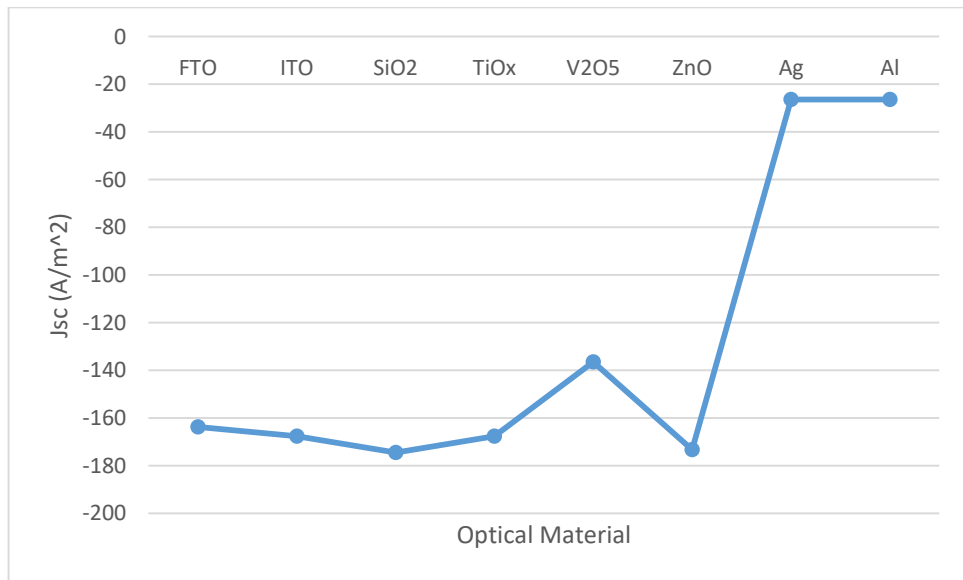


Figure 21: J_{sc} variation over optical materials

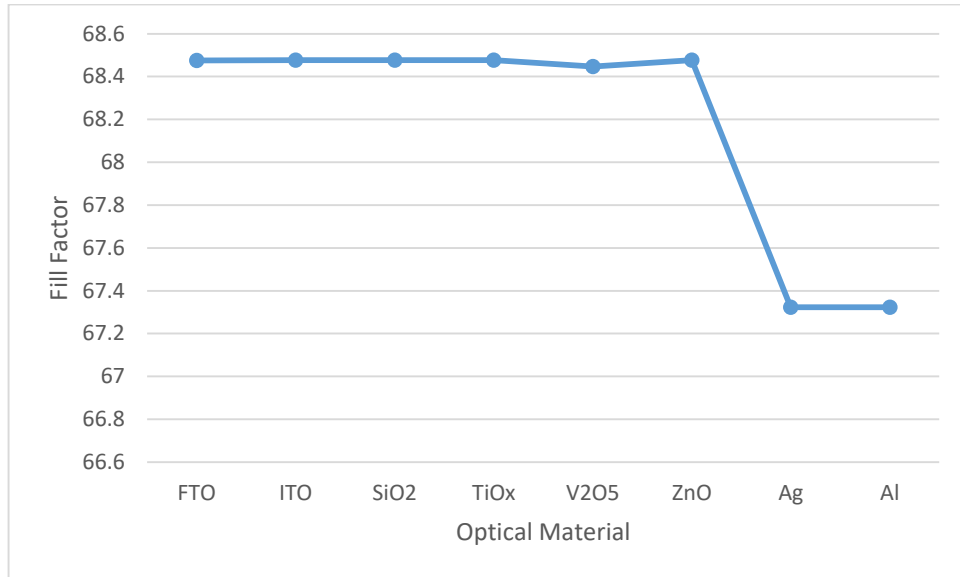


Figure 22: Fill factor variation over optical materials

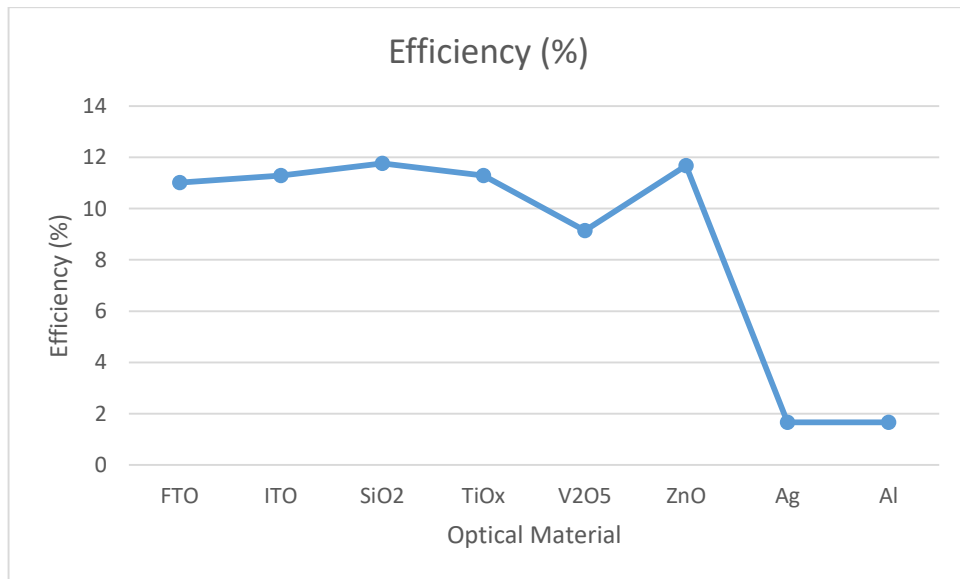


Figure 23: Efficiency variation over optical materials

Solar cells require highly conductive front and back contacts to facilitate the transport of electrons and holes out of the device. Usually a metal is used as the back contact. As a result for this work Ag was used as the back contact. Aluminium (Al) gives results close to Ag when simulated as back contact, but since silver is known to be the most conductive metal, it was chosen. The front contact needs to be transparent as well as conductive to allow light into the cell. Thus the oxides are a better choice. Metals are less transparent, hence results with Ag and Al show very low efficiency and voltage output.

Moreover the optimum band gap plays an essential role in the performance of a solar cell as denoted by the PCE [27], because the band gap has a direct effect on V_{oc} . Increasing band gap to an optimum value increases V_{oc} , thus improving the activity of cell. In light of this fact, which of the oxides perform better depends a lot on their respective band gap values. SiO_2 performs the best due to its very high band gap value (table 11). Second to SiO_2 is ZnO . Even though ITO comes third, it is usually more preferred due to its high fill factor value, where fill factor is a parameter which along with V_{oc} and J_{sc} determines the maximum power from a solar cell [33]. Given that the tandem cell already has a layer of silicon as active layer, another additional layer of silicon is not necessary. Although it would improve efficiency, it would also add to the cost of the device.

Table 11: Band gaps of oxides

Optical material	FF	Efficiency (%)	Band gap (eV)
FTO	68.474787	11.017688	3.86
ITO	68.477234	11.286384	3.5 to 4.3
SiO_2	68.476243	11.758627	8.4 to 11.0
TiO_x	68.477234	11.286384	~3.2 to 3.35
V_2O_5	68.447638	09.141130	~2.2 to 2.4
ZnO	68.476737	11.675120	~3.37

As seen in figure 24, the efficiency of a silicon base cell with FTO as front contact is only around 1.48%, as opposed to a perovskite/Si tandem cell with the same front contact having an efficiency of around 11.02%. This proves that tandem cells are more efficient. Tandem cells utilise the idea of splitting the spectrum and utilise multiple band gaps. In this case, the tandem cell can utilise the perovskite at the top to absorb high energy photons, while it can utilise the silicon at the bottom to absorb low energy photons.


```

Voc= 0.305269 (V)
Jsc= -67.588227 (A/m^2)
Pmax= 14.788025 (W/m^2)
Pmax Voltage= 0.239257 (V)
FF= 71.673079
Efficiency= 1.478802 percent

```

Figure 24: Simulation result for Voc, Jsc, Pmax, Pmax Voltage, fill factor (FF) and power conversion efficiency for Si base solar cell

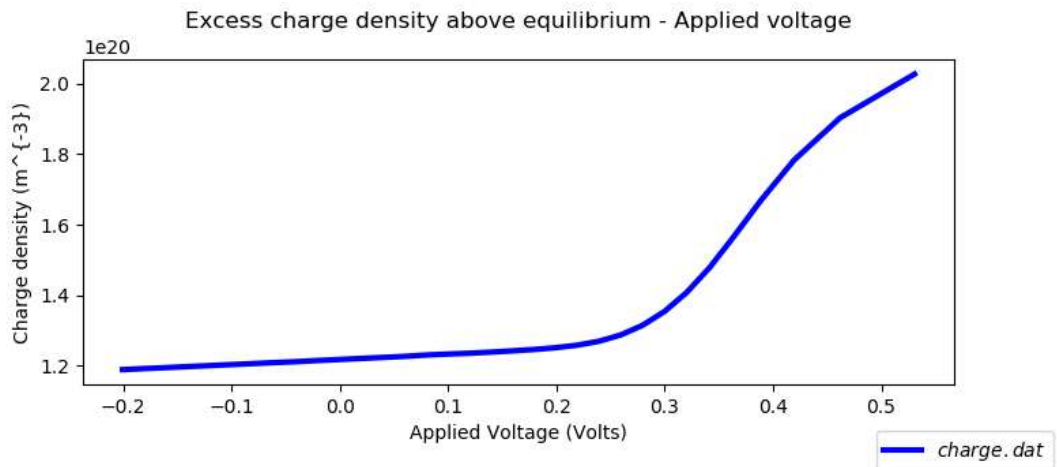


Figure 25: Charge density vs. Applied voltage

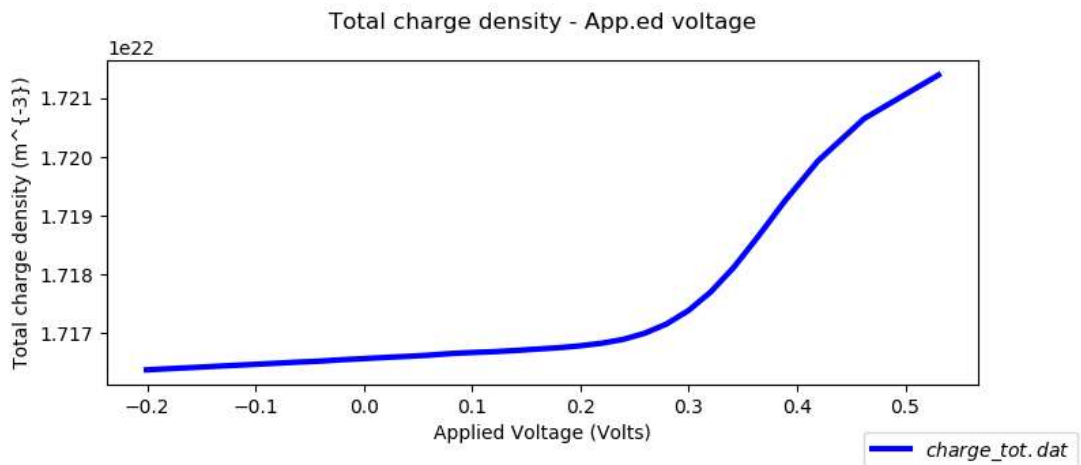


Figure 26: Total charge density vs. Applied voltage

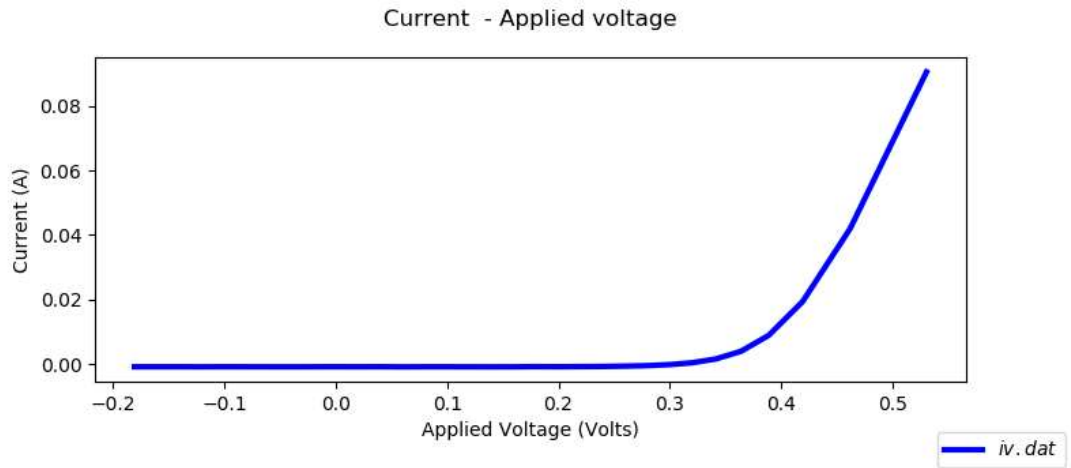


Figure 27: Current vs. Applied voltage

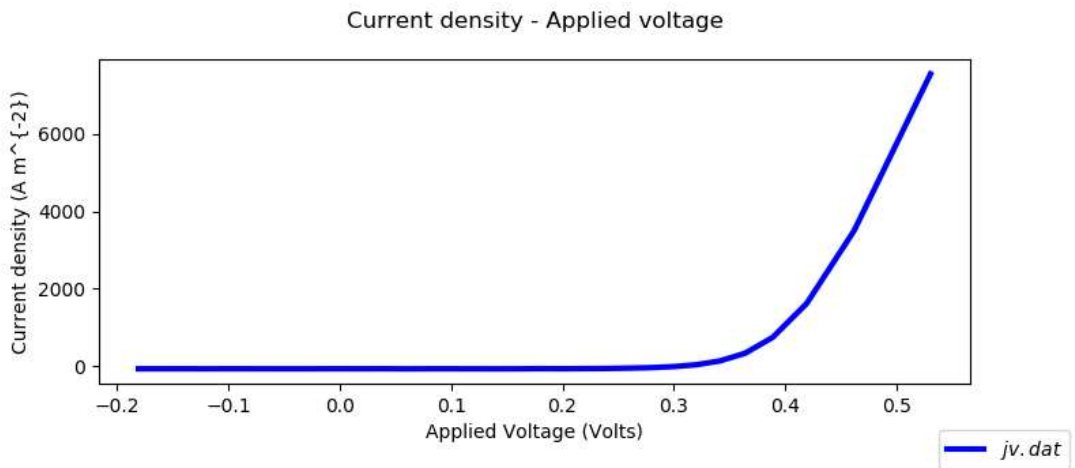


Figure 28: Current density vs. Applied voltage

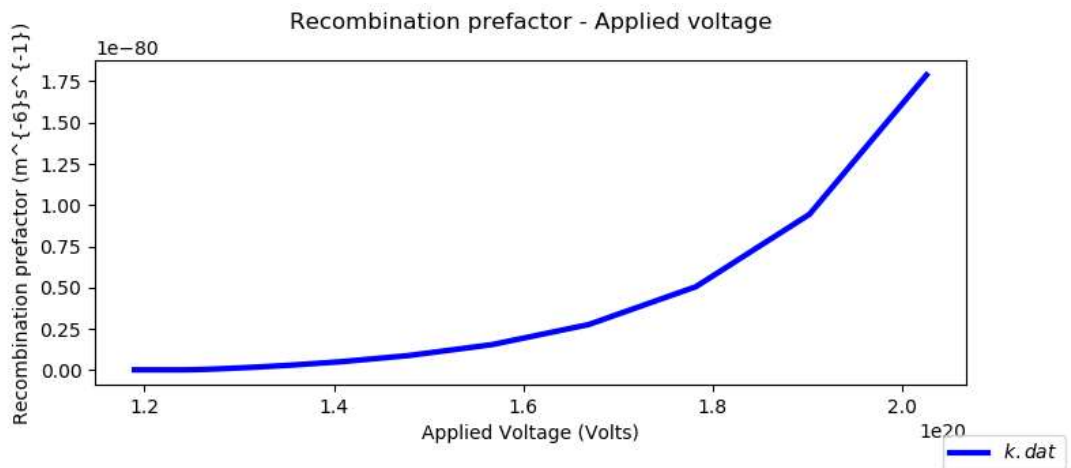


Figure 29: Recombination prefactor vs. Applied voltage

Table 12: Simulation information

Fill factor	0.716731	a.u.
Power conversion efficiency	1.478802	Percent
Max power	14.788025	Wm ⁻²
V _{oc}	0.305269	V
Recombination time constant at V _{oc}	1.364358e61	s
Recombination rate at V _{oc}	1.032192e-41	m ⁻³ s ⁻¹
Average carrier density at P _{max}	1.269690e+20	m ⁻³
Recombination time constant	1.184187e+62	m ⁻¹
Trapped electrons at V _{oc}	0.000000e+00	m ⁻³
Trapped holes at V _{oc}	0.000000e+00	m ⁻³
Free electrons at V _{oc}	1.706996e+22	m-3
Free holes at V _{oc}	1.728408e+22	m-3
J _{sc}	-6.758823e+01	Am-2
Total carriers (n+p)/2 at V _{oc}	3.424697e+22	m-3
Current density at max power	-6.180814e+01	Am-2
Voltage at max power	2.392569e-01	V

Chapter 5 Summary and Conclusions

This thesis concludes that ZnO and ITO are the most suitable optical materials for use as front contact in a perovskite/Si tandem solar cell. Their suitability is mainly due to

- Their band gap values
- Conductivity
- Transparency
- Fill factor

SiO₂ was found to be the best performer, however additional silicon based material in a solar cell would add to the cost.

From the comparison between the tandem solar cell and simple silicon based solar cell's performances, it can be concluded that a tandem cell is more efficient, which was also proved in literature. This is mainly due to the ability of the tandem cell to split the spectrum and utilising multiple band gaps within its active layers, such that there is more photon absorption and less photon wastage in the device, making the process more efficient.

The quantitative results were not satisfactory due to the software related issues as discussed in validation, however the qualitative analysis shows that the results are in coherence with the practical results of solar cells.

Chapter 6 Future Directions and Recommendations

As per the challenges and inadequacies faced during this study, the following recommendations could be made for researchers pursuing this field of study in the future.

- Commercialisation of perovskite solar cells is still a challenge in terms of fabrication and stability, so there is scope to conduct experimentation regarding fabrication processes. Some processes have been mentioned in literature.
- Tandem perovskite/Si cells have progressed rapidly with efficiencies already above 25% in some cases, so there is a possibility of more improvement if research continues.
- More studies should be conducted on composite materials for use in the layers of tandem cells. Polymers have proven to be very efficient according to literature.
- Studies can be conducted to find optimised contact pairs, i.e. front and back contacts that perform the best with each other.
- Older versions of the GPVDM software (version 5.0) allow material addition, so for new material study, version 8 (as such used for this thesis) is not a proper choice. The software itself needs more improvement and debugging, so it is suggested to conduct more research and inform the issues faced regarding the software to Dr. MacKenzie to aid in software development. Dr. McKenzie's contact details are available within the software interface and he responds to emails swiftly.
- Alternative software, especially software with hardware sets such as SCAPS-1D, are a very good choice for such research, since the results from simulation can be validated against the experimental results.

References

- [1] “Perovskites Solar Cell Structure, Efficiency & More | Ossila.” [Online]. Available: <https://www.ossila.com/pages/perovskites-and-perovskite-solar-cells-an-introduction#ref6>. [Accessed: 07-Mar-2021].
- [2] M. A. Green, Y. Hishikawa, E. D. Dunlop, D. H. Levi, J. Hohl-Ebinger, and A. W. Y. Ho-Baillie, “Solar cell efficiency tables (version 52),” *Prog. Photovoltaics Res. Appl.*, vol. 26, no. 7, pp. 427–436, 2018.
- [3] “Perovskite Solar | Perovskite-Info.” [Online]. Available: <https://www.perovskite-info.com/perovskite-solar>. [Accessed: 07-Mar-2021].
- [4] “Perovskite solar cell: Hero, villain or just plain fantasy?” [Online]. Available: <https://www.solarpowerworldonline.com/2020/02/perovskite-solar-cells-hero-villain-or-just-plain-fantasy/>. [Accessed: 07-Mar-2021].
- [5] “Oxford PV closes £65 million funding round | Perovskite-Info.” [Online]. Available: <https://www.perovskite-info.com/oxford-pv-closes-65-million-funding-round>. [Accessed: 07-Mar-2021].
- [6] “Dyesol declares perovskite stability breakthrough | Perovskite-Info.” [Online]. Available: <https://www.perovskite-info.com/dyesol-declares-perovskite-stability-breakthrough>. [Accessed: 07-Mar-2021].
- [7] “solar cell | Definition, Working Principle, & Development | Britannica.” [Online]. Available: <https://www.britannica.com/technology/solar-cell#ref289540>. [Accessed: 11-Mar-2021].
- [8] R. Amantea, “An introduction to modeling and simulation,” *R.C.A. Rev.*, vol. 46, no. 3, pp. 281–288, 1985.
- [9] A. De Vos, “Detailed balance limit of the efficiency of tandem solar cells,” *J. Phys. D. Appl. Phys.*, vol. 13, no. 5, pp. 839–846, May 1980.
- [10] J. Xu *et al.*, “Triple-halide wide-band gap perovskites with suppressed phase segregation for efficient tandems,” *Science (80-.)*, vol. 367, no. 6482, pp. 1097–1104, 2020.

- [11] Y. Hou *et al.*, “Efficient tandem solar cells with solution-processed perovskite on textured crystalline silicon,” *Science* (80-.), vol. 367, no. 6482, pp. 1135–1140, 2020.
- [12] B. Chen *et al.*, “Blade-Coated Perovskites on Textured Silicon for 26%-Efficient Monolithic Perovskite/Silicon Tandem Solar Cells,” *Joule*, vol. 4, no. 4, pp. 850–864, 2020.
- [13] M. Jošt, L. Kegelmann, L. Korte, and S. Albrecht, “Monolithic Perovskite Tandem Solar Cells: A Review of the Present Status and Advanced Characterization Methods Toward 30% Efficiency,” *Adv. Energy Mater.*, vol. 10, no. 26, 2020.
- [14] J. P. Mailoa *et al.*, “A 2-terminal perovskite/silicon multijunction solar cell enabled by a silicon tunnel junction,” *Appl. Phys. Lett.*, vol. 106, no. 12, 2015.
- [15] J. Werner *et al.*, “Zinc tin oxide as high-temperature stable recombination layer for mesoscopic perovskite/silicon monolithic tandem solar cells,” *Appl. Phys. Lett.*, vol. 109, no. 23, pp. 2–6, 2016.
- [16] Y. Wu *et al.*, “Monolithic perovskite/silicon-homojunction tandem solar cell with over 22% efficiency,” *Energy Environ. Sci.*, vol. 10, no. 11, pp. 2472–2479, 2017.
- [17] J. Zheng *et al.*, “Large area efficient interface layer free monolithic perovskite/homo-junction-silicon tandem solar cell with over 20% efficiency,” *Energy Environ. Sci.*, vol. 11, no. 9, pp. 2432–2443, 2018.
- [18] J. Zheng *et al.*, “21.8% Efficient Monolithic Perovskite/Homo-Junction-Silicon Tandem Solar Cell on 16 cm²,” *ACS Energy Lett.*, vol. 3, no. 9, pp. 2299–2300, 2018.
- [19] D. Rached and R. Mostefaoui, “Influence of the front contact barrier height on the Indium Tin Oxide/hydrogenated p-doped amorphous silicon heterojunction solar cells,” *Thin Solid Films*, vol. 516, no. 15, pp. 5087–5092, 2008.
- [20] M. Stolterfoht, V. M. Le Corre, M. Feuerstein, P. Caprioglio, L. J. A. Koster, and D. Neher, “Voltage-Dependent Photoluminescence and How It Correlates

- with the Fill Factor and Open-Circuit Voltage in Perovskite Solar Cells,” *ACS Energy Lett.*, vol. 4, no. 12, pp. 2887–2892, 2019.
- [21] E. L. Unger *et al.*, “Hysteresis and transient behavior in current-voltage measurements of hybrid-perovskite absorber solar cells,” *Energy Environ. Sci.*, vol. 7, no. 11, pp. 3690–3698, 2014.
- [22] R. Cheacharoen, N. Rolston, D. Harwood, K. A. Bush, R. H. Dauskardt, and M. D. McGehee, “Design and understanding of encapsulated perovskite solar cells to withstand temperature cycling,” *Energy Environ. Sci.*, vol. 11, no. 1, pp. 144–150, 2018.
- [23] K. Ellmer, R. Wendt, and R. Cebulla, “ZnO/ZnO:Al window and contact layer for thin film solar cells: high rate deposition by simultaneous rf and dc magnetron sputtering,” *Conf. Rec. IEEE Photovolt. Spec. Conf.*, pp. 851–854, 1996.
- [24] M. F. Ali and M. F. Hossain, “Influence of Front and Back Contacts on Photovoltaic Performances of p-n Homojunction Si Solar Cell: Considering an Electron-Blocking Layer,” *Int. J. Photoenergy*, vol. 2017, 2017.
- [25] S. Ahmed *et al.*, “Simulation studies of Sn-based perovskites with Cu back-contact for non-toxic and non-corrosive devices,” *J. Mater. Res.*, vol. 34, no. 16, pp. 2789–2795, 2019.
- [26] Afrasiab *et al.*, “Optimization of efficient monolithic perovskite/silicon tandem solar cell,” *Optik (Stuttg.)*, vol. 208, no. January, p. 164573, 2020.
- [27] M. Aitezaz Hussain, S. Khan, A. Rahim, A. Jan, and M. Rashid, “Optimization of Power Conversion Efficiency for Perovskite Solar Cell using GPVDM,” *Int. J. Eng. Work.*, vol. 07, no. 02, pp. 109–115, 2020.
- [28] W. Farooq *et al.*, “Thin-Film Tandem Organic Solar Cells with Improved Efficiency,” *IEEE Access*, vol. 8, pp. 74093–74100, 2020.
- [29] M. Sittirak, J. Ponrat, K. Thubthong, P. Kumnorkaew, J. Lek-Uthai, and Y. Infahsaeng, “The effects of layer thickness and charge mobility on performance of FAI:MABr:PbI₂:PbBr₂ perovskite solar cells: GPVDM simulation

approach,” *J. Phys. Conf. Ser.*, vol. 1380, no. 1, 2019.

- [30] A. Hima, N. Lakhdar, B. Benhaoua, A. Saadoune, I. Kemerchou, and F. Rogti, “An optimized perovskite solar cell designs for high conversion efficiency,” *Superlattices Microstruct.*, vol. 129, no. March, pp. 240–246, 2019.
- [31] R. Yasodharan, A. P. Senthilkumar, J. Ajayan, and P. Mohankumar, “Effects of layer thickness on Power Conversion Efficiency in Perovskite solar cell: A numerical simulation approach,” *2019 5th Int. Conf. Adv. Comput. Commun. Syst. ICACCS 2019*, pp. 1132–1135, 2019.
- [32] “Spiro-OMeTAD (Spiro-MeOTAD) | CAS 207739-72-8 | Ossila.” [Online]. Available: <https://www.ossila.com/products/spiro-ometad?variant=23115455681>. [Accessed: 12-Mar-2021].
- [33] “Fill Factor | PVEducation.” [Online]. Available: <https://www.pveducation.org/pvcdrom/solar-cell-operation/fill-factor>. [Accessed: 13-Mar-2021].